

Identification of Imidazo[1,2-b]pyridazine derivatives as Potent, Selective, and Orally Active Tyk2 JH2 Inhibitors

Chunjian Liu, James Lin, Ryan Moslin, John S Tokarski, Jodi K. Muckelbauer, ChiehYing Chang, Jeffrey Tredup, Dianlin Xie, Hyunsoo Park, Peng Li, Dauh-Rung Wu, Joann Strnad, Adriana Zupa-Fernandez, Lihong Cheng, Charu Chaudhry, Jing Chen, Cliff Chen, Huadong Sun, Paul Elzinga, Celia D'arienzo, Kathleen M. Gillooly, Tracy L. Taylor, Kim W. McIntyre, Luisa Salter-Cid, Louis J Lombardo, Percy H Carter, Nelly Aranibar, James R. Burke, and David S. Weinstein

ACS Med. Chem. Lett., **Just Accepted Manuscript** • DOI: 10.1021/acsmedchemlett.9b00035 • Publication Date (Web): 21 Feb 2019

Downloaded from <http://pubs.acs.org> on February 22, 2019

Just Accepted

“Just Accepted” manuscripts have been peer-reviewed and accepted for publication. They are posted online prior to technical editing, formatting for publication and author proofing. The American Chemical Society provides “Just Accepted” as a service to the research community to expedite the dissemination of scientific material as soon as possible after acceptance. “Just Accepted” manuscripts appear in full in PDF format accompanied by an HTML abstract. “Just Accepted” manuscripts have been fully peer reviewed, but should not be considered the official version of record. They are citable by the Digital Object Identifier (DOI®). “Just Accepted” is an optional service offered to authors. Therefore, the “Just Accepted” Web site may not include all articles that will be published in the journal. After a manuscript is technically edited and formatted, it will be removed from the “Just Accepted” Web site and published as an ASAP article. Note that technical editing may introduce minor changes to the manuscript text and/or graphics which could affect content, and all legal disclaimers and ethical guidelines that apply to the journal pertain. ACS cannot be held responsible for errors or consequences arising from the use of information contained in these “Just Accepted” manuscripts.



	Lombardo, Louis; Bristol-Myers Squibb Research, Immunology Chemistry Carter, Percy; BMS, R&D Aranibar, Nelly; Bristol-Myers Squibb Pharmaceutical Research and Development Burke, James; Bristol-Myers Squibb Pharmaceutical Research and Development, Metabolism and Pharmacokinetic Department, Pharmaceutical Candidate Optimization Weinstein, David; Bristol Myers Squibb Co, Discovery Chemistry

SCHOLARONE™
Manuscripts

Identification of Imidazo[1,2-b]pyridazine derivatives as Potent, Selective, and Orally Active Tyk2 JH2 Inhibitors

Chunjian Liu*, James Lin, Ryan Moslin, John S. Tokarski, Jodi Muckelbauer, ChiehYing Chang, Jeffrey Tredup, Dianlin Xie, Hyunsoo Park, Peng Li, Dauh-Rurng Wu, Joann Strnad, Adriana Zupa-Fernandez, Lihong Cheng, Charu Chaudhry, Jing Chen, Cliff Chen, Huadong Sun, Paul Elzinga, Celia D'ariento, Kathleen Gillooly, Tracy L. Taylor, Kim W. McIntyre, Luisa Salter-Cid, Louis J. Lombardo, Percy H. Carter, Nelly Aranibar, James R. Burke, and David S. Weinstein

Department Research & Development, Bristol-Myers Squibb, P.O. Box 5400, Princeton, New Jersey 08543, United States

KEYWORDS: *Tyk2 JH2 inhibitor(s), Tyk2 JH2 ligand(s), Tyk2 pseudokinase inhibitor(s), Tyk2 pseudokinase ligand(s)*

ABSTRACT: In sharp contrast to a previously reported series of 6-anilino imidazopyridazine based Tyk2 JH2 ligands, 6-((2-oxo-N1-substituted-1,2-dihydropyridin-3-yl)amino)imidazo[1,2-b]pyridazine analogs were found to display dramatically improved metabolic stability. The N1-substituent on 2-oxo-1,2-dihydropyridine ring can be a variety of alkyl, aryl and heteroaryl groups, but among them, 2-pyridyl provided much enhanced Caco-2 permeability, attributed to its ability to form intramolecular hydrogen bonds. Further SAR studies at the C3 position led to the identification of highly potent and selective Tyk2 JH2 inhibitor **6**, which proved to be highly effective in inhibiting IFN γ production in a rat pharmacodynamics model and fully efficacious in a rat adjuvant arthritis model.

Tyrosine kinase 2 (Tyk2), a member of the Janus kinase (JAK) family of non-receptor tyrosine kinases, regulates the phosphorylation of Signal Transducer and Activation of Transcription (STAT) proteins downstream of the receptors for the p40-containing cytokines IL-12 and IL-23 as well as Type I interferons such as IFN α , IFN β , resulting in the activation of STAT-dependent transcription and functional responses specific for these receptors.¹⁻³ These receptor signaling pathways play key roles in the pathogenesis of autoimmune and inflammatory diseases. IL-12 and IL-23 were found at high levels in lesional skin of psoriatic patients,⁴⁻⁶ and the expression of these cytokines were shown to decrease after various treatments that provide symptomatic relief in psoriasis.^{7,8} Elevated serum IFN α levels were observed in Systemic Lupus Erythematosus (SLE) patients,⁹ and the levels correlated to both disease activity and severity.¹⁰ Inhibition of both IL-12 and IL-23 by targeting their common p40 subunit with ustekinumab (Stelara[®]), proved to be clinically effective for the treatment of psoriasis^{11,12} and Crohn's disease,^{13,14} and ustekinumab was approved by FDA for the treatment of these diseases. Targeting IFN α as a potential therapeutic solution to SLE was also validated by the Phase IIb results from anifrolumab, a human monoclonal antibody that binds to and blocks the receptor for Type I interferons.^{15,16} Meanwhile, Tyk2 deficient mice were reported to be resistant to collagen-induced arthritis (CIA) and experimental autoimmune encephalomyelitis (EAE).^{17,18} Thus, Tyk2 has been rationalized as a promising target for developing orally active therapeutic agents for autoimmune and inflammatory disorders¹⁹.

As the Janus kinase family is named after the two faced Roman god Janus, the structures of Tyk2 and other Jak family members feature dual kinase domains proximal to each other, a catalytic kinase domain and a pseudokinase domain, also called Jak homology 1 (JH1) and Jak homology 2 (JH2), respectively. The Tyk2 JH2 is capable of binding adenosine triphosphate (ATP), but it is catalytically incompetent.²⁰ However, Tyk2 JH2 has been shown to play an important regulatory role in Tyk2 function.²¹ Tyk2 JH1 inhibitors such as **1**²² and **2**²³ (Figure 1) have been reported. Due to the high degree of homology among the JH1 of all Jak family members, it is not surprising that **1** and **2** display only moderate Tyk2 selectivity, as they also show significant activities against Jak1-3.

In order to target the Tyk2 dependent signaling pathway more selectively, we focused on Tyk2 JH2 due to its unique structural difference in the binding pocket compared to JH1 and have recently disclosed the identification of Tyk2 JH2 ligand **3** (Figure 2) through a chemogenomic approach.²⁴ This Tyk2 JH2 ligand does not bind to Tyk2 JH1 and exhibits high selectivity over other kinases including other Jak family members. Moreover, **3** is effective in blocking the activation of Tyk2 JH1. 6-Anilino imidazopyridazines (IZP) **4** represents another chemotype of Tyk2 JH2 ligands that we have preliminarily reported most recently.²⁵ The structure-activity relationship (SAR) for this series was investigated, but the extremely poor metabolic stability remained a formidable issue. For example, after 10 minutes of incubation of **4** in human, rat, and mouse liver microsomes, the remaining **4** was found to be only 11%, 14%, and 1%, respectively. Previous

effort to address the metabolic stability issue led to **5**, which displayed much improved liver microsomal stability with 99%, 76%, and 44% recoveries in human, rat, and mouse, respectively. However, unfortunately, it showed very limited permeability, indicated by its low Caco-2 value of 34 nm/sec, and subsequently very limited exposure in vivo. Now, we would like to report our modification of the 6-anilino IZP series into 6-(2-oxo-N1-substituted-1,2-dihydropyridin-3-yl)amino IZP, represented by **6**. Tyk2 JH2 inhibitor **6** not only dramatically improved the metabolic stability but it also proved to be orally bioavailable, highly effective in inhibiting IFN γ in rat, and fully efficacious in a rat adjuvant arthritis (AA) model at a low dose (5 mg/kg, bid).

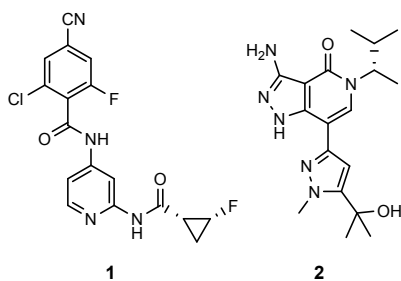


Figure 1. Literature Tyk2 JH1 inhibitors **1** and **2**

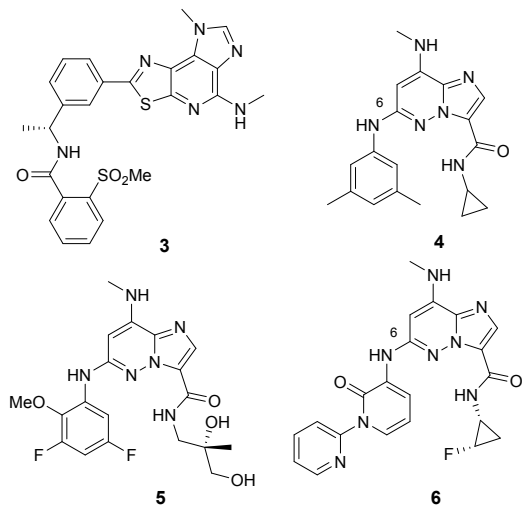


Figure 2. Tyk2 JH2 inhibitors **3-6**

The much improved liver microsomal stability for compound **5**, compared to **4**, is most likely due to its much reduced cLogP of 1.99, calculated by ChemBioDraw Ultra 14.0, versus 3.80 for **4**. It is well known that decreasing cLogP can improve metabolic stability.²⁶ The limited permeability observed for **5** may be understandable considering that the molecule carries five H-bond donors (three NH and two OH groups). Searching for a moiety that can effectively reduce cLogP without introducing too much polarity, we wondered if the anilino group in **4** could be replaced with 2-oxo-N1-substituted-1,2-dihydropyridin-3-ylamino functionality. Thus, **6a**, the calculated cLogP of which is 0.66, was synthesized. The compound turned out to be approximately 6 fold less potent against Tyk2 JH2 compared to **4** based on their Ki determinations (Table 1). It was also less potent by about 6 fold than **4** in the IFN α stimulated luciferase reporter assay in Kit225 T cells. The human whole blood (hWB) activity for **6a** was not obtained due to its poor solubility in

this assay. However, to our satisfaction, **6a** displayed significantly improved liver microsomal stability. After 10 minutes of incubation in human, rat, and mouse liver microsomes, the remaining **6a** was found to be 56%, 63%, and 10%, respectively, versus only 11%, 14%, and 1% for **4** (The liver microsomal stability and Caco-2 data for all analogs are arranged in Table I in the Supporting Information). More encouragingly, when the N-methyl on the pyridone ring in **6a** was substituted with cyclopropyl, the liver microsomal stability for **6b** was further improved, with the recoveries now being 88%, 71%, and 39%, respectively. Its Tyk2 JH2 binding affinity and cellular activity were also improved to be comparable to that for **4**. Further more, Tyk2 JH2 ligand **6b** was found to be active in hWB assay with its IC₅₀ being determined to be 817 nM. Use of an aryl group such as paracyanophenyl on the pyridone resulted in **6c**, which improved the metabolic stability further to the incubation recoveries of 92%, 77%, and 71% from human, rat, and mouse liver

Table 1. The SAR observed for R¹ with **6a-m**

compd	R1	Tyk2 JH2 Ki (nM)	IFN α IC ₅₀ (nM)	hWB IC ₅₀ (nM)
4	NA	0.13	96	ND
6a	Me	0.74	614	ND
6b	cPr	0.33	131	817
6c	NC-C ₆ H ₄	0.20	90	268
6d	Me-C(O)Me-C ₆ H ₄	0.07	111	811
6e	Pyridin-2-yl	0.34	94	398
6f	F-C ₆ H ₄	0.14	140	380
6g	Pyridin-3-yl	0.29	148	346
6h	F-C ₆ H ₄	0.22	70	371
6i	F-C ₆ H ₄	0.15	99	236
6j	F-C ₆ H ₄	0.12	61	313
6k	F-C ₆ H ₄	0.38	235	464
6l	Me-C ₆ H ₄	0.091	147	247
6m	Me-C ₆ H ₄	0.48	135	340

microsomes, respectively. Analog **6c** displayed an hWB IC₅₀ of 268 nM, 3 fold more active than what was observed for **6b**, although its Tyk2 JH2 affinity and cellular functional activity were only slightly better.

A co-crystal structure of **6c** bound to Tyk2 JH2 was obtained,²⁷ and the binding mode was revealed to be the same

as that for a 6-anilino IZP ligand.²⁵ Namely, **6c** interacts with Tyk2 JH2 protein mainly through two hydrogen bond networks (Figure 3). One occurs at the hinge region involving hydrogen bonds between the C8 methylamino NH and the carbonyl of Val690 and between N1 of the IZP core and the NH of Val690. The other takes place near the gatekeeper involving hydrogen bonds from the C3 amide carbonyl to the NH of Lys642 and to the carbonyl of Glu688 through a bridging water molecule. The pyridone ring is sandwiched between the p-loop and Pro694, with the cyanophenyl pointing to a solvent exposed area, which may mean a relatively flat SAR for R¹. It is noted that the cyanophenyl and pyridone rings are almost perpendicular with the dihedral angle between the two rings being 85.1°.

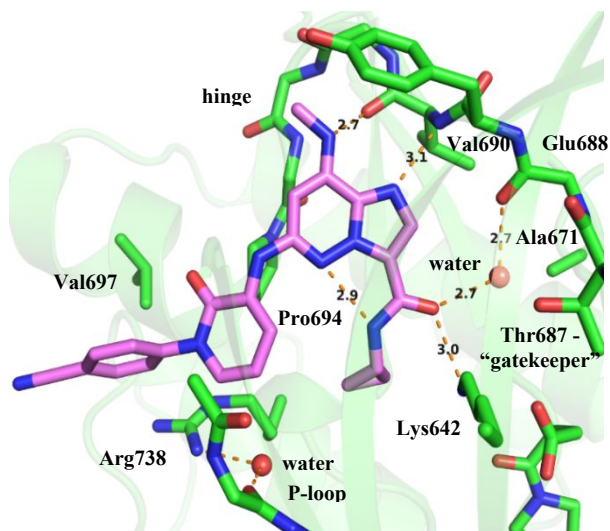


Figure 3. Co-crystal structure of **6c** bound to Tyk2 JH2

While **6c** looked promising for its activities and metabolic stability, its extremely low aqueous solubility (< 1 µg/mL at pH 6.5 and 2 µg/mL at pH 1.0) was a concern. Replacement of the cyano in **6c** with a solubilizing group such as carbinol (**6d**) led to significant loss of Caco-2 permeability. As a result, we turned our focus to the exploration of N1-heteroaryl-2-oxo-1,2-dihydropyridin-3-yl analogs. 2''-, 3''-, 4''-Pyridyl analogs **6e**, **6f**, and **6g** all provided Tyk2 JH2 enzymatic, cellular, and hWB activities similar to what were obtained for **6c**. The major differentiation among the three compounds came from their Caco-2 permeability, with **6e** (Caco-2 = 169 nm/sec) being significantly more permeable than **6f** and **6g** (Caco-2 = 51 and 38 nm/sec, respectively). It should be mentioned that the Caco-2 data were found to correlate very well with in vivo exposures for the current series, and a relatively high Caco-2 value was crucial for desired exposure. In spite of knowing that the cyanophenyl and pyridone rings were perpendicular in **6c** in its co-crystal structure with Tyk2 JH2, we speculated that the 2''-pyridyl in **6e** could be significantly more co-planar to the pyridone ring, due to two potential intramolecular hydrogen bonds: from the pyridyl nitrogen to the proximal hydrogen on the pyridone ring and from pyridone oxygen to the proximal hydrogen on the 2''-pyridyl. Intramolecular hydrogen bonding interactions involving aromatic C-H are known in literature.²⁸ As a result, the 2''-pyridyl nitrogen and the pyridone oxygen in **6e** would be shielded by the intramolecular hydrogen bonds and therefore the molecule would be significantly less polar and

more permeable compared to **6f** and **6g**. The speculation was confirmed by single-crystal X-ray analyses of **6e**. Two conformers resulted from rotations of the single bond between the pyridine and pyridone rings were observed, and one of them is shown in Figure 4. The dihedral angles between the two heteroaryl rings is measured to be 34.8°, which is significantly smaller than what (85.1°) was observed between the cyanophenyl and pyridone rings in **6c**. And, the speculated intramolecular H-bonds are conceivable. The pyridyl and pyridone rings in the other conformer²⁹ are also more coplanar (dihedral angle = 51.1°), though less significantly, than the cyanophenyl and pyridone rings in **6c**. The afore-discussed intramolecular hydrogen bonding interactions in the second conformer may be less significant, but the more coplanar first conformer can certainly account for the much higher Caco-2 permeability observed for **6e**, considering the two conformers will be in equilibrium in solution. Metabolically, **6e** is also more stable in the rodent liver microsomes than **6f** and **6g**. On the basis of **6e**, three fluorinated 2''-pyridyl analogs **6h**, **6i**, and **6j** were prepared. All three compounds displayed very similar activity results to that for **6e**. Interestingly, only **6h** and **6i** remained highly permeable as **6e**. The Caco-2 of 59 nm/sec for **6j** was more like what was found for **6f** and **6g**. It can be rationalized that due to the presence of 6''-F on the pyridine in **6j**, the pyridyl and pyridone rings will be less co-planar and more polar (lack of potential intramolecular hydrogen bonds), compared to **6h** and **6i**. Among the other heteroaryls on the pyridone ring examined, pyrimidyl and pyridazinyl were suitable to provide activities and liver microsomal stability comparable to that for **6e**, but the Caco-2 results for **6k** and **6l** were in the low to moderate range. On the other hand, dimethylpyrazole derived analog **6m** was found to be highly permeable (Caco-2 = 142 nm/sec) in addition to showing good activities and liver microsomal stability.

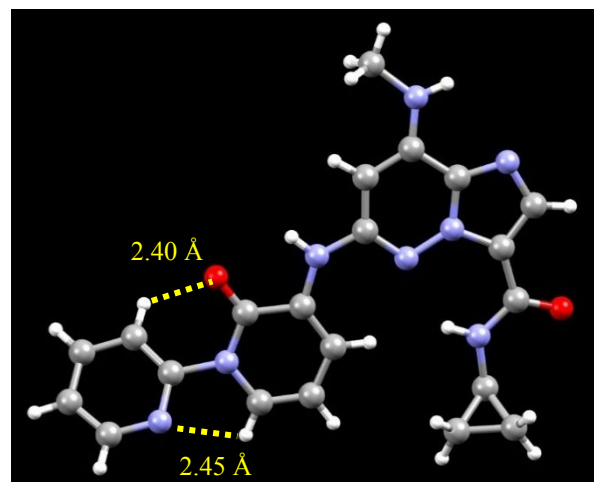
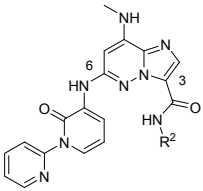


Figure 4. Single crystal structure of **6e**

Table 2 presents the SAR results observed for R² of the C3 amide side chain with R¹ being fixed to be 2-pyridyl. Replacement of the N-cyclopropyl in **6e** with N-isopropyl appeared to improve the Tyk2 JH2 binding affinity by 2 or 3 fold, but the cellular and hWB activities for **6n** were slightly less potent than that for **6e**. The cyclobutyl analog **6o** displayed approximately the same potencies as **6e** in all three assays. A larger substitution such as 3-hydroxy-2,2-dimethylpropyl was also well tolerated, as **6p** was shown to

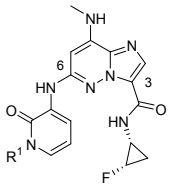
be equipotent to **6e**. The best finding for R² was the enantiomeric (1R, 2S)-2-fluorocyclopropyl group, which enhanced the Tyk2 JH2 affinity by 4 fold, as inhibitor **6** exhibited a K_i of 0.086 nM. The enhancement in enzymatic potency led to the same level of improvement in its cellular and hWB activities.

Table 2. The SAR observed for R² with **6e**, **6n-p**, and **6**



compd	R ²	Tyk2 JH2 K _i (nM)	IFN α IC ₅₀ (nM)	hWB IC ₅₀ (nM)
6e	cPr	0.34	94	382
6n	iPr	0.13	153	750
6o	cBu	0.26	60	384
6p		0.29	84	285
6		0.086	25	81

Table 3. The SAR observed for R¹ with **6** and **6q-t**

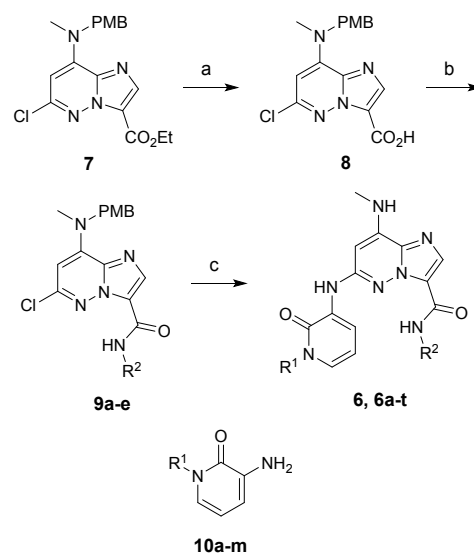


compd	R ¹	Tyk2 JH2 K _i (nM)	IFN α IC ₅₀ (nM)	hWB IC ₅₀ (nM)
6		0.086	25	81
6q		0.035	26	85
6r		0.024	12	136
6s		0.015	22	90
6t		0.018	41	63

Combining (1R, 2S)-2-fluorocyclopropyl, the best group identified for R², with some of the preferred R¹ from Table 1 prompted the synthesis of **6q-t** (Table 3). As expected, these compounds were highly potent inhibitors of Tyk2 JH2, with their K_i values in the range of 0.015 to 0.035 nM. The K_i values appeared to suggest that **6q-t** would be somewhat more potent inhibitors than **6**, but in the cellular and hWB assays they behaved very similarly to **6**, with IFN α and hWB IC₅₀ values in the ranges of 12 to 41 nM and 63 to 136 nM, respectively. The liver microsomal stability for these compounds were reasonable except for **6q**. It was noticed that all the (1R, 2S)-2-fluorocyclopropyl analogs showed reduced Caco-2 permeability to some extent, compared to their corresponding des-fluorocyclopropyl counterparts.

Compounds **6** and **6a-t** were synthesized according to Scheme 1, using a previously reported advanced intermediate **7**²⁵ (Scheme 1). Hydrolysis of **7** provided IZP carboxylic acid **8**, which was then converted to carboxamide **9a-e** by benzotriazole-1-ylxytris(dimethylamino)phosphonium hexafluorophosphate (BOP) promoted coupling reactions. Buchwald reactions of **9a-e** with aminopyridone **10a-m**, catalyzed by tris(dibenzylideneacetone)dipalladium(0)/xantphos or Pd(OAc)₂/BrettPhos, followed by the removal of the p-methoxybenzyl (PMB) protection group, gave rise to **6** and **6a-t**.

Scheme 1^a. Synthesis of **6**, **6a-t**



^aReagent and conditions: (a) LiOH, MeOH/THF, rt, 2 h, 97%; (b) R¹NH₂, BOP, N, N-diisopropylethylamine, rt, 16 h, 55-97%; (c) i. **10a-m**, tris(dibenzylideneacetone)dipalladium(0)/xantphos/Cs₂CO₃ or Pd(OAc)₂/BrettPhos/K₂CO₃, 1,4-dioxane, 80-125 °C, 2-3 h, ii. HCl/1,4-dioxane, CH₂Cl₂, rt, 30 min, 6-46% over 2 steps.

Throughout the SAR studies, several compounds were selected for pharmacokinetic (PK) studies, and it was found that **6** exhibited the most desired PK profiles. The PK results for **6** in mouse, rat, cyno, and dog are summarized in Table 4. In brief, **6** displayed a low clearance rate of 7.8 mL/min/kg in rat and moderate clearance rates of 16, 17, and 25 mL/min/kg in mouse, cyno, and dog, respectively. It provided the highest oral exposure and bioavailability (114%) in rat among the four species examined. The bioavailability observed in mouse, cyno, and dog were 86%, 46%, and 50%, respectively.

Table 4^{a,b}. PK profiles for **6** in mouse, rat, cyno, and dog

species	mouse	rat	cyno	dog
Dose (PO) (mg/kg)	10	10	10	10
C _{max} (μM)	15	9.4	1.8	0.93
AUC _{0-24h} (μM*h)	19	57	11	8.0
CL (mL/min/kg)	16	7.8	17	25
F (%)	86	114	46	50

^aVehicle: 5:5:90 TPGS:EtOH:PEG300; ^bIV dose: 2 mg/kg

Tyk2 JH2 inhibitor **6** was then evaluated in a pharmacodynamic (PD) model to inhibit IL-12/IL-18 induced IFN γ production. In this study, **6** was first administered to rats,

and after one hour, the rats were challenged with IL-12. Another hour later, they were further challenged with IL-18. Five hours after drug administration, plasma samples were collected and analyzed for IFN γ levels. As shown in Figure 5, **6** was effective in a dose dependent manner in this model, inhibiting IL-12/IL-18 induced IFN γ production by 45% and 77% at doses of 1 and 10 mg/kg, respectively.

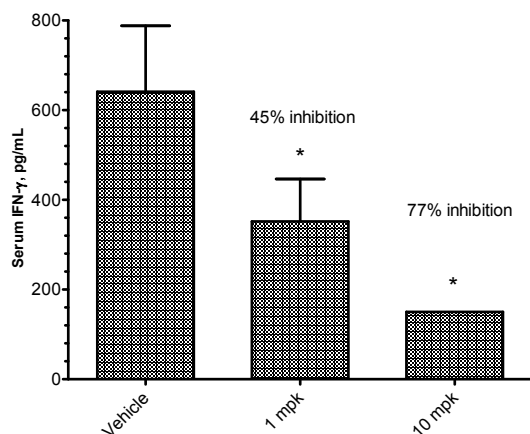


Figure 5. Inhibitor **6** in the IL12 + IL18 induced IFN γ in rats (Vehicle: 5:5:90 TPGS:EtOH:PEG300)

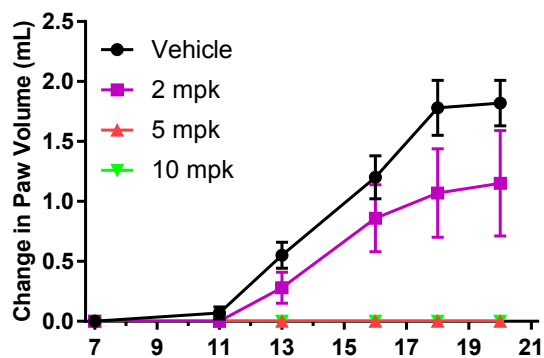


Figure 6. Inhibitor **6** in the rat adjuvant arthritis model (bid dosing; vehicle: 5:5:90 TPGS:EtOH:PEG300)

Compound **6** was also shown to be highly efficacious in a rat adjuvant arthritis (rat AA) model. In this study, adjuvant was given to rats on day zero for the rats to develop arthritis. Meanwhile, **6** was dosed to the rats, twice a day, from day zero to day twenty, during which period the rats' paw volumes were periodically measured. As seen in Figure 6, **6** demonstrated full efficacy to prevent the rats' paw from swelling at bid doses of 5 and 10 mg/kg.

It should be mentioned that **6** proved to be remarkably selective over other kinases, displaying > 10,000 fold selectivity for Tyk2 JH2 over a diverse panel of 230 kinases that include Tyk2 JH1 and other Jak family members. HIPK4 is the only kinase, over which **6** showed a selectivity of only 480 fold. More specifically, **6** inhibited Jak1-3 with IC₅₀ values of > 2 μ M and displayed the Jak1-3 dependent cellular activities of > 12.5 μ M (IC₅₀ values).

In summary, a 2-oxo-1-substituted-1,2-dihydropyridin-3-ylamino moiety was identified as a viable replacement for the anilino group of a previously reported series of 6-anilino

imidazopyridazine based Tyk2 JH2 ligands to dramatically improve metabolic stability. A variety of N1-heteroaryl groups on the 2-oxo-1,2-dihydropyridin-3-yl were found appropriate for Tyk2 JH2 activity, but it was 2-pyridyl that provided the desired Caco-2 permeability due to its ability to form intramolecular hydrogen bonds. Further SAR studies led to the identification of highly potent and selective Tyk2 JH2 inhibitor **6**. Compound **6** displayed good to excellent PK profiles among the species of mouse, rat, monkey, and dog. It was highly effective in a pharmacodynamic (PD) model to inhibit IL-12/IL-18 induced IFN γ production in rat, and fully efficacious in a preventive rat adjuvant arthritis (rat AA) model at a dose of 5 mg/kg.

ASSOCIATED CONTENT

Supporting Information

The Supporting Information containing experimental procedures and characterization for all final compounds, as well as descriptions of in vitro and in vivo studies, is available free of charge on the ACS Publications website.

AUTHOR INFORMATION

Corresponding Author

*Tel: +1 609 466 5101; E-mail: chunjian.liu@bms.com.

Notes

The authors declare no competing financial interest.

ACKNOWLEDGMENT

The authors would like to acknowledge Richard Rampulla and the BBRC DDS group for supply of intermediates.

REFERENCES

- (1) Sohn, S. J.; Barrett, K.; Van Abbema, A.; Chang, C.; Kohli, P. B.; Kanda, H.; Smith, J.; Lai, Y.; Zhou, A.; Zhang, B.; Yang, W.; Williams, K.; MacLeod, C.; Hurley, C. A.; Kulagowski, J. J.; Lewin-Koh, N.; Dengler, H. S.; Johnson, A. R.; Ghilardi, N.; Zak, M.; Liang, J.; Blair, W. S.; Magnuson, S.; Wu, L. C. A Restricted Role for TYK2 Catalytic Activity in Human Cytokine Responses Revealed by Novel TYK2-Selective Inhibitors. *J. Immunol.* **2013**, *191*, 2205–2216.
- (2) Ghoreschi, K.; Laurence, A.; O'Shea, J. J. Janus Kinases in Immune Cell Signaling. *Immunol. Rev.* **2009**, *228*, 273–287.
- (3) Shuai, K.; Liu, B. Regulation of JAK-STAT Signaling in the Immune System. *Nat. Rev. Immunol.* **2003**, *3*, 900–911.
- (4) Piskin, G.; Sylva-Steenland, R. M. R.; Bos, J. D.; Teunissen, M. B. M. In vitro and in situ expression of IL-23 by keratinocytes in healthy skin and psoriasis lesions: enhanced expression in psoriatic skin. *J. Immunol.* **2006**, *176*, 1908–1915.
- (5) Lee, E.; Trepicchio, W. L.; Oestreicher, J.; Pittman, D.; Wang, F.; Chamian, F.; Dhodapkar, M.; Krueger, J. G. Increased expression of interleukin 23p19 and p40 in lesional skin of patients with psoriasis vulgaris. *J. Exp. Med.* **2004**, *199*, 125–130.
- (6) Yawalkar, N.; Karlen, S.; Hunger, R.; Brand, C. U.; Braathen, L. R. Expression of interleukin-12 is increased in psoriatic skin. *J. Invest. Dermatol.* **1998**, *111*, 1053–1057.
- (7) Tada, Y.; Asahina, A.; Takekoshi, T.; Kishimoto, E.; Mitsui, H.; Saeki, H.; Komine, M.; Tamaki, K. Interleukin 12 production by monocytes from patients with psoriasis and its inhibition by cyclosporin A. *Br. J. Dermatol.* **2006**, *154*, 1180–1183.
- (8) Piskin, G.; Tursen, U.; Sylva-Steenland, R. M.; Bos, J. D.; Teunissen, M. B. M. Clinical improvement in chronic plaque-type psoriasis lesions after narrow-band UVB therapy is accompanied by

a decrease in the expression of IFN γ inducers - IL-12, IL-18 and IL-23. *Exp. Dermatol.* **2004**, *13*, 764–772.

(9) Kim, T.; Kanayama, Y.; Negoro, N.; Okamura, M.; Takeda, T.; Inoue, T. Serum levels of interferons in patients with systemic lupus

erythematosus. *Clin Exp Immunol.* **1987**, *70*, 562–9.

(10) Bengtsson, A. A.; Sturfelt, G.; Truedsson, L.; Blomberg, J.; Alm, G.; Vallin, H.; Rönnblom, L. Activation of type I interferon system in systemic lupus erythematosus correlates with disease activity but not with antiretroviral antibodies. *Lupus* **2000**, *9*, 664–71. (b) Dall'era, M. C.; Cardarelli, P. M.; Preston, B. T.; Witte, A.; Davis Jr, J. C. Type I interferon correlates with serologic and clinical manifestations of systemic lupus erythematosus. *Ann. Rheum. Dis.* **2005**, *64*, 1692–1697.

(11) Kimball, A. B.; Gordon, K. B.; Fakhrazadeh, S.; Yeilding, N.; Szapary, P. O.; Schenkel, B.; Guzzo, C.; Li, S.; Papp, K. A. Long-term efficacy of ustekinumab in moderate-to-severe psoriasis: results from the PHOENIX 1 trials through up to 3 years. *Br. J. Dermatol.* **2012**, *166*, 861–872.

(12) Papp, K. A.; Langley, R. G.; Lebwohl, M.; Krueger, G. G.; Szapary, P.; Yeilding, N.; Guzzo, C.; Hsu, M.-C.; Wang, Y.; Li, S.; Dooley, L. T.; Reich, K. Efficacy and safety of ustekinumab, a human interleukin-12/23 monoclonal antibody, in patients with psoriasis: 52-week results from a randomized, double-blind, placebo controlled trial (PHOENIX 2). *Lancet* **2008**, *371*, 1675–1684.

(13) Sandborn, W. J.; Gasink, C.; Gao, L. L.; Blank, M. A.; Johanns, J.; Guzzo, C.; Sands, B. E.; Hanauer, S. B.; Targan, S.; Rutgeerts, P.; Ghosh, S.; de Villiers, W. J.; Panaccione, R.; Greenberg, G.; Schreiber, S.; Lichtiger, S.; Feagan, B. G., and CERTIFI Study Group. Ustekinumab induction and maintenance therapy in refractory Crohn's disease. *N. Engl. J. Med.* **2012**, *367*, 1519–1528.

(14) Sandborn, W. J.; Feagan, B.; Fedorak, R. N.; Scherl, E.; Fleisher, M. R.; Katz, S.; Johanns, J.; Blank, M.; Rutgeerts, P. A randomized trial of ustekinumab, a human interleukin-12/23 monoclonal antibody, in patients with moderate-to-severe Crohn's disease. *Gastroenterology* **2008**, *135*, 1130–1141.

(15) Sciascia, S.; Talavera-Garcia, E.; Roccatello, D.; Baldovino, S.; Mengatti, E.; Cuadrado, M. J. Upcoming biological therapies in systemic lupus erythematosus. *Int. Immunol.* **2015**, *27*, 189–193.

(16) Mathian, A.; Hie, M.; Cohen-Aubart, F.; Amoura, Z. Targeting Interferons in Systemic Lupus Erythematosus: Current and Future Prospects. *Drugs* **2015**, *75*, 835–846.

(17) Ortmann, R.; Smeltz, R.; Yap, G.; Sher, A., and Shevach, E. M. A heritable defect in IL-12 signaling in B10.Q/J mice. I. In vitro analysis. *J. Immunol.* **2001**, *166*, 5712–5719.

(18) Oyamada, A.; Ikebe, H.; Itsumi, M.; Saiwai, H.; Okada, S.; Shimoda, K.; Iwakura, Y.; Nakayama, K. I.; Iwamoto, Y.; Yoshikai, Y., and Yamada, H. Tyrosine kinase 2 plays critical roles in the pathogenic CD4 T cell responses for the development of experimental autoimmune encephalomyelitis. *J. Immunol.* **2009**, *183*, 7539–7546.

(19) Liang, Y.; Zhu, Y.; Xia, Y.; Peng, H.; Yang, X.-K.; Liu, Y.-Y.; Xu, W.-D.; Pan, H.-F.; Ye, D.-Q. Therapeutic potential of tyrosine kinase 2 in autoimmunity. *Expert Opin Ther targets.* **2014**, *18*, 571–80.

(20) Min, X.; Ungureanu, D.; Maxwell, S.; Hammarén, H.; Thibault, S.; Hillert, E.-K. Ayres, M.; Greenfield, B.; Eksterowicz, J.; Gabel, C.; Walker, N.; Silvennoinen, O.; and Wang, Z. Structural and Functional Characterization of the JH2 Pseudokinase Domain of JAK Family Tyrosine Kinase 2 (TYK2). *J. Biol. Chem.* **2015**, *290*, 27261–27270.

(21) Staerk, J.; Kallin, A.; Demoulin, J. B.; Vainchenker, W., and Constantinescu, S. N. JAK1 and Tyk2 activation by the homologous polycythemia vera JAK2 V617F mutation: cross-talk with IGF1 receptor. *J. Biol. Chem.* **2005**, *280*, 41893–41899.

(22) Liang, J.; van Abbema, A.; Balazs, M.; Barrett, K.; Berezhkovsky, L.; Blair, W.; Chang, C.; Delarosa, D.; DeVoss, J.; Driscoll, J.; Eigenbrot, C.; Ghilardi, N.; Gibbons, P.; Halladay, J.; Johnson, A.; Kohli, P. B.; Lai, Y.; Liu, Y.; Lyssikatos, J.; Mantik, P.; Menghrajani, K.; Murray, J.; Peng, I.; Sambrone, A.; Shia, S.; Shin, Y.; Smith, J.; Sohn, S.; Tsui, V.; Ultsch, M.; Wu, L. C.; Xiao, Y.;

Yang, W.; Young, J.; Zhang, B.; Zhu, B.-y.; Magnuson, S. Lead Optimization of a 4-Aminopyridine Benzamide Scaffold To Identify Potent, Selective, and Orally Bioavailable TYK2 Inhibitors. *J. Med. Chem.* **2013**, *56*, 4521–4536.

(23) Yogo, T.; Nagamiya, H.; Seto, M.; Sasaki, S.; Shih-Chung, H.; Ohba, Y.; Tokunaga, N.; Lee, G. N.; Rhim, C. Y.; Yoon, C. H.; Cho, S. Y.; Skene, R.; Yamamoto, S.; Satou, Y.; Kuno, M.; Miyazaki, T.; Nakagawa, H.; Okabe, A.; Marui, S.; Aso, K.; Yoshida, M. Structure-Based Design and Synthesis of 3-Amino-1,5-dihydro-4H-pyrazolopyridin-4-one Derivatives as Tyrosine Kinase 2 Kinases. *J. Med. Chem.* **2016**, *59*, 733–749.

(24) Tokarski, J. S.; Zupa-Fernandez, A.; Tredup, J. A.; Pike, K.; Chang, C. Y.; Xie, D.; Cheng, L.; Pedicord, D.; Muckelbauer, J.; Johnson, S. R.; Wu, S.; Edavettal, S. C.; Hong, Y.; Witmer, M. R.; Lisa L. Elkin, L. L.; Blat, Y.; Pitts, W. J.; Weinstein, D. S.; Burke, J. R. Tyrosine Kinase 2-mediated Signal Transduction in T Lymphocytes Is Blocked by Pharmacological Stabilization of Its Pseudokinase Domain. *J. Biol. Chem.* **2015**, *290*, 11061–11074.

(25) Moslin, R.; Gardner, D.; Santella, J.; Zhang, Y.; Duncia, J.; Liu, C.; Lin, J.; Tokarski, J.; Strnad, J.; Pedicord, D.; Chen, J.; Blat, Y.; Zupa-Fernandez, A.; Cheng, L.; Sun, H.; Chaudhry, C.; Huang, C.; D'Arienzo, C.; Sack, J. S.; Muckelbauer, J. K.; Chang, C.; Tredup, J.; Xie, D.; Aranibar, N.; Burke, J. R.; Carter, P. H. and Weinstein, D. S. Identification of imidazo[1,2-b]pyridazine TYK2 pseudokinase ligands as potent and selective allosteric inhibitors of TYK2 signaling. *MedChemComm.* **2017**, *8*, 700–712.

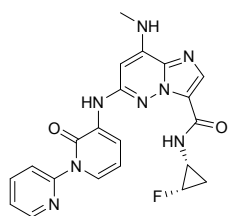
(26) Nassar, A.-E. F.; Kamel, A. M.; Clarimont, C. Improving the decision-making process in the structural modification of drug candidates: enhancing metabolic stability. *Drug Discov. Today.* **2004**, *9*, 1020–1028.

(27) PDB 6NSL.

(28) Niebel, C.; Lokshin, V.; Sigalov, M.; Krief, P.; Khodorkovsky, V. Intra- and intermolecular C(sp²)-O hydrogen bonds in a series of isobenzofuranone derivatives: manifestation and energetics. *Eur. J. Org. Chem.* **2008**, *21*, 3689–3699.

(29) CCDC 1893350.

1
2
3
4 For Table of Contents Use Only



Tyk2 JH2 K_i = 0.086 nM

IFN α IC_{50} = 25 nM

hWB IC_{50} = 81 nM

effective in inhibiting IFN γ production in rats

efficacious in a rat adjuvant arthritis model